Early metal smelting in Aksum, Ethiopia: copper or iron?

Thorsten SEVERIN[1], Thilo REHREN[2,*] and Helmut SCHLEICHER[1]

[1] Mineralogisch-Petrographisches Institut der Universität Hamburg, Grindelallee 48, 20146 Hamburg, Germany
[2] UCL Qatar, PO Box 23689, Education City, Doha, Qatar
*Corresponding author, e-mail: th.rehren@ucl.ac.uk

Abstract: A selection of archaeometallurgical remains from the 3rd/4th century A.D., found in Aksum, Ethiopia, were analysed in order to determine the nature of the process by which they were produced, *i.e.* copper or iron smelting. Chemical and mineralogical analyses excluded a relationship to copper smelting; instead, all samples are consistent with a highly efficient iron smelting operation using the bloomery process and slag tapping furnaces. A lateritic iron ore containing at least 80 wt% FeO was smelted, resulting in an estimated one unit by weight of iron metal produced for every unit by weight of slag left behind, and little erosion of furnace wall material. The zoning of spinels, with chromium- and aluminium-rich inner parts and mixed hercynitic-ulvitic outer rims, reflects the evolution of the melt phase under strongly reducing conditions.

Key-words: archaeometallurgy, iron, copper, smelting, Aksum, Ethiopia, archaeology, slag, mass balance estimate.

1. Introduction

Our knowledge of metal smelting technology in pre-colonial sub-Saharan Africa is incomplete, and heavily biased towards iron smelting. The rather sporadic evidence of copper smelting reported so far (*e.g.*, Tylecote, 1982; Childs & Killick, 1993; Miller *et al*., 2001; Miller, 2002; Miller & Killick, 2004) is mostly restricted to the western and southern part of the continent, and does not support the notion of a widespread Copper or Bronze Age preceding iron smelting in Africa, even though copper artefacts, mostly of a decorative nature and synchronous with iron artefacts, are known from the archaeological record. Thus, the suggested identification of copper smelting in the 3rd to 4th century A.D. at Aksum, Ethiopia (Ziegert, 2001, 2006, 2009), sparked considerable interest and provided the basis for the study presented here. In this study, we analysed 19 samples of ore, furnace wall fragments, furnace slag and tap slag collected and provided by Ziegert for this purpose, using established chemical and mineralogical methods of archaeometallurgical analysis.

The city of Aksum is located on the plateau of Tigray (*ca.* 2100 m above sea level), in the north-western highlands of Ethiopia, about 50 km from the border to Eritrea (Fig. 1).

Founded around A.D. 100 by Zoskales, Aksum quickly became the centre of a major empire, well connected with trade routes exploiting its strategic geographical position (Munroe-Hay, 1991). This geographic advantage led to a period of prosperity in the 3rd and 4th century A.D., a period during which Aksum controlled a large area of land, including the trade routes going northwards along the Nile and eastwards up to the Red Sea. Commercial relations with the Roman and Byzantine Empires were established; even connections with India and Sri Lanka are known. In the 3rd century A.D. the Aksumitic kingdom was an empire comparable to the Roman and Persian ones (Munroe-Hay, 1991). During the reign of Ezana in the early 4th century A.D., the population of Aksum converted to Christianity. The city started to decline in the 7th century.

The existence of a small but rich copper occurrence in Debarwa, in present-day Eritrea, on the route between Aksum and Asmara is of relevance for this paper. While this was briefly exploited in the 1960's, there are no reports known of ancient mining in this region. Furthermore, various iron ore deposits are scattered throughout both Eritrea and Ethiopia, some of which were exploited in the mid-20th century. As with the copper ore, however, no reports of ancient mining are known for any of these deposits.

This study has several aims: firstly, to test whether the copper smelting postulated by Ziegert (2001, 2006, 2009) can be confirmed by archaeometallurgical analysis of slag finds from the furnace site; secondly, to reconstruct the metallurgical process represented by these slags; and thirdly, to estimate the quantity of metal produced based on the amount of slag preserved at the site.

2. Materials and methods

In 1994 and again in 1998–2001, excavations in Aksum revealed within a larger settlement the remains of at least
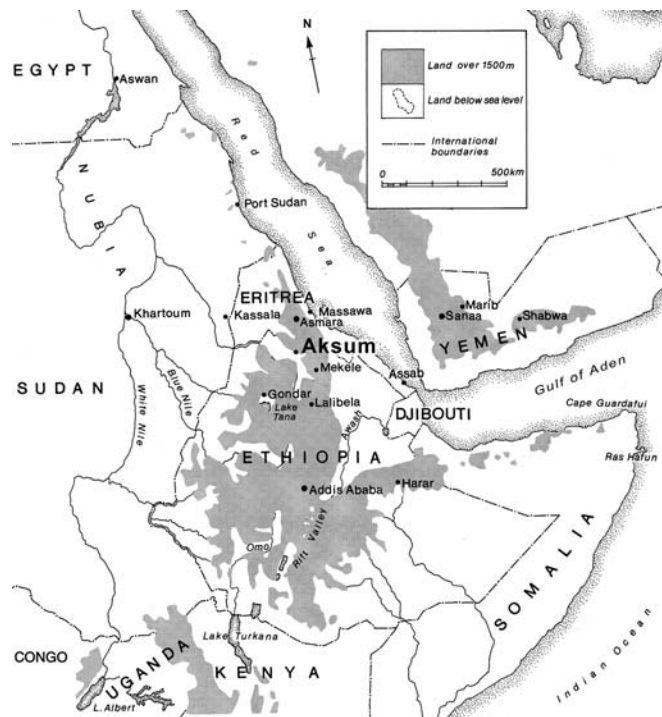
Fig. 1. Location of the town of Aksum on the Tigray plateau in modern-day Ethiopia.

one furnace, together with slag and ore fragments, all covered by a volcanic tuff layer dated to 325 A.D. (Ziegert, 2001, 2006, 2009, Ziegert, pers. comm. 2003). In 2003, the excavator provided 19 metallurgical samples which he had selected in the field for export and analysis. All 19 samples were prepared as polished thin sections for transmitted and reflected polarised light optical microscopy and electron probe micro-analysis (EPMA), using a Cameca SX 100. The measurements, at 15 kV accelerating voltage and 20 nA beam current, included the following elements: Na, K, Ca, Ba, Al, Si, Mg, P, Ti, Mn, Fe, Cr, and Ni. Count times were set at 20 s for peak positions and 10 s for background positions. Simple minerals and pure oxides were used to calibrate count rates for each element, and an andradite standard was used to monitor instrument drift during analysis; none was found. The analytical error is thought to be around 1 % relative for elements present at above c 10 wt%, while detection limits for elements above atomic number 12 are around 0.05 wt% or lower. For low concentrations and light elements analytical errors and detection limits increase.

For bulk chemical composition determination, X-ray fluorescence (XRF) analyses of all samples were carried out using a Spectro Xlab Pro 2000 (P)ED-XRF. For these analyses, the samples were cleaned of all adhering contamination, incorporated sand grains were removed mechanically as far as possible, and then the samples were crushed and ground to below 50 μm grain size. The powdered material was dried for 16 hours at 105 °C, then mixed with synthetic wax at a ratio by weight of 8–0.8989, and pressed into a pellet. The analytical protocol for the

(P)ED-XRF instrument, developed for iron-rich slag powder matrices (see Veldhuijzen, 2003, 2005 for full details), uses a sequence of four secondary targets to generate incident X-rays optimised for different excitation conditions within the analytical spectrum, ranging from 55 kV tube voltage for the Al_2O_3 secondary target to 10 kV for the HOPG secondary target. A Co target was added to the standard line-up of three secondary targets to enhance detection limits for transition elements within the iron-rich matrix. Each pellet was measured three times to check for precision; the data reported here represent the averages of those three individual measurements (Table 1). Additionally, a certified reference material (BCS 381) was measured to verify the accuracy of the results; accuracy was found to be better than two percent relative for oxides present at or above 10 wt%, while the light elements magnesium and aluminium were not well detected and relative errors increase significantly for elements present at low concentrations (Table 1). The oxide values were recalculated to 100 wt% to facilitate comparison with literature data. Oxygen was not determined analytically, but calculated by stoichiometry both for EPMA and XRF analyses, assuming all iron to be present as Fe^{2+}.

The preliminary macroscopic identification of the slag samples followed Sperl (1980) and Bachmann (1982), assessing morphology, colour, porosity, magnetism, and density. Four different types of material were identified, namely ore (samples 315a 1–3), ceramic furnace wall material with attached slag (302d 1 + 2, 313f, 313g 1 + 2, and 314), furnace slag (samples 302a, 302c, and 313a), and tap slag (samples 302b, 313c, 313d, 313e, 314a, 315b, 315c).

3. Results and discussion

The ore pieces are rounded, about 5 cm in diameter and red. They consist mostly of haematite, goethite and quartz (Fig. 2). The ore shows no reaction to a hand-held magnet. The identification of this material as ore occurred in the field by the archaeologist, prior to analysis, presumably based on its apparent difference from the surrounding geology and its association with the smelting remains. It was thought to represent either ore left over from storage, or accidentally lost during the process, or more likely discarded at the last minute by the smelter as being of inferior quality. We therefore cannot be certain that it is representative of the material smelted here, but are confident that it is at least a close approximation. Part of the interpretation of the analytical results aims to test this hypothesis, by comparing the composition of this presumed ore to that of the produced slag.

The furnace slags are dark grey to olive green, with flow textures surrounding charcoal fragments and leaving a typical surface pattern of charcoal impressions (Fig. 3). When sectioned, they appear relatively more porous than the tapped slags (see below). They are rusty in some areas, but are not magnetic. Their maximum size varies from 5 to 9 cm, the density is between 4.10 and 4.23 g/cm^3 and the

Table 1. Composition of slag, furnace wall material and ore samples from Aksum, Ethiopia, and a certified reference material (BCS 381, Basic Slag) determined by (P)ED-XRF. The data is sorted by decreasing iron oxide content within each group of material. All data recalculated to 100 wt%. bdl = below detection limit. Mixed = sample consists of a mixture of slag and furnace wall material. FeO as FeOtot.

Element	SiO_2 (wt%)	TiO_2 (wt%)	Al_2O_3 (wt%)	FeO (wt%)	MnO (wt%)	MgO (wt%)	CaO (wt%)	K_2O (wt%)	Na_2O (wt%)	P_2O_5 (wt%)	SO_3 (wt%)	V_2O_5 (wt%)	Co (ppm)	Cu (ppm)	Zn (ppm)	Sr (ppm)	Zr (ppm)	Ba (ppm)	Ce (ppm)	Pb (ppm)
302c furnace slag	33.6	0.94	7.2	54.5	0.06	0.29	2.15	0.27	0.42	0.24	0.18	0.16	160	50	25	210	380	170	50	200
302a furnace slag	34.6	0.95	6.6	53.9	0.07	0.28	2.28	0.24	0.54	0.26	0.17	0.16	170	30	20	230	410	180	40	200
313a furnace slag	34.7	0.95	6.8	53.3	0.07	0.30	2.58	0.30	0.52	0.20	0.17	0.16	170	30	20	240	400	180	50	190
313c tap slag	27.2	1.08	6.9	61.8	0.04	0.14	1.68	0.22	0.38	0.19	0.25	0.13	160	35	25	250	340	130	45	240
313e tap slag	28.0	1.06	6.7	61.3	0.05	0.15	1.54	0.19	0.42	0.18	0.21	0.14	200	30	25	240	370	120	40	250
314a tap slag	31.4	0.98	7.4	57.1	0.06	0.34	1.43	0.32	0.43	0.24	0.19	0.14	210	50	40	180	340	160	bdl	220
302b tap slag	31.8	0.96	7.4	56.7	0.06	0.22	1.35	0.29	0.60	0.17	0.21	0.14	140	40	30	170	360	180	60	210
315c tap slag	32.7	0.96	7.9	55.5	0.06	0.15	1.34	0.30	0.65	0.16	0.22	0.14	150	25	35	170	350	200	40	210
313d tap slag	32.7	1.02	8.4	53.8	0.06	0.33	2.09	0.42	0.55	0.25	0.19	0.13	140	30	30	230	340	180	45	200
315b tap slag	36.7	0.92	7.2	50.9	0.07	0.37	2.02	0.47	0.71	0.26	0.18	0.15	170	35	25	220	370	270	35	190
302d.2 slag	34.7	0.91	7.6	51.8	0.06	0.24	3.17	0.37	0.59	0.21	0.16	0.15	160	20	25	280	400	200	50	190
302d.1 slag	34.8	0.90	7.5	51.3	0.07	0.27	3.56	0.39	0.60	0.31	0.15	0.15	160	35	25	300	390	210	45	190
313g.1 mixed	47.6	0.75	9.0	36.2	0.06	0.47	3.31	1.43	0.77	0.24	0.07	0.09	120	35	45	290	320	560	45	100
313g.2 mixed	53.1	0.73	11.5	26.8	0.10	0.48	3.98	1.54	1.38	0.27	0.11	0.07	100	35	40	380	340	610	70	60
314 furnace wall	65.1	0.86	15.4	9.0	0.10	1.08	3.03	2.62	1.96	0.73	0.10	0.02	70	30	40	320	320	960	90	20
313f furnace wall	70.4	0.67	16.5	3.8	0.08	0.86	2.12	3.10	2.34	0.08	0.04	0.01	70	20	75	280	270	1040	85	20
315a-1 ore	14.2	0.46	3.7	80.2	0.05	bdl	0.25	0.00	bdl	0.81	0.13	0.08	110	40	bdl	bdl	150	90	30	bdl
315a-3 ore	15.5	0.43	6.7	75.0	0.04	bdl	0.36	0.02	0.31	1.29	0.19	bdl	170	45	85	30	140	80	bdl	bdl
315a-2 ore	17.9	0.46	7.3	72.0	0.06	0.02	0.36	0.03	0.29	1.16	0.15	bdl	170	40	80	30	160	110	bdl	bdl
BCS 381 meas.	9.32	0.31	0.10	17.95	3.19	bdl	50.57	0.05	0.71	16.00	0.66	0.91	26	7	13	319	30	423	bdl	27
BCS 381 given	9.15	0.36	0.70	17.82	3.29	1.07	51.05	–	–	16.36	0.50	–	–	–	–	–	–	–	–	–

Fig. 2. Ore sample 315a.

Fig. 3. Furnace slag sample 302c.

Fig. 4. (a), (b) Tap slag sample 313e, top and bottom surfaces.

mass ranges from ∼100 to 250 g. This type of slag most likely solidified inside the furnace within a bed of charcoal pieces.

The tap slag has an obvious flow texture with a characteristic surface resembling the solidified flows of a viscous melt (Fig. 4a) and very low internal porosity. With a thickness of only 1–2.5 cm, these samples are much thinner compared to the furnace slags. Their lower surface is characterised by occasional incorporated sand grains and numerous small dimples, most likely sand grain impressions (Fig. 4b). This indicates a flow of the slag over a

rough and sandy ground. Tap slag constitutes the largest part of the analysed assemblage, with seven pieces compared to only three furnace slag samples. Unfortunately, we do not know whether this is representative of the relative proportion of slag types at the excavation, or is due to a sampling bias favouring such pieces.

Several samples of slag were intimately intergrown with heavily vitrified ceramic material, most likely fragments of the furnace wall in direct contact with the slag melt. Cutting reveals a clear boundary between slag and furnace wall material, and shows the latter to be very rich in quartz fragments (Fig. 5). As in the case of the furnace and tapped slags, these samples are not magnetic, but show a higher porosity. Analysis of this mixed slag and ceramic material was carried out to understand the potential contribution of incorporated furnace wall material to the slag formation. The composition of these samples varies widely, reflecting the intimate intergrowths of furnace wall material and slag which was impossible to fully separate prior to preparation of the powder for analysis. Thus, these fragments of intergrown ceramic and slag serve as a proxy for a slag which has absorbed significant parts of furnace wall material.

Fig. 5. Cross section through furnace wall material (right) with adhering slag (left); sample 313 g. Note the abundant quartz inclusions (white) in the ceramic part of the sample.

3.1. Slag formation

The smelting of ore in antiquity can be seen as a sequence of solid state and liquid state chemical reactions taking place under strongly reducing conditions at ambient air pressure and temperatures of up to *ca.* 1300 °C. The purpose of the process is the formation of metal from the metal oxides present in the ore, which requires that it takes place under very low oxygen partial pressures in an atmosphere rich in carbon monoxide. The formation and development of slag from the fusion of the materials in the furnace charge is governed by similar principles as the formation of magmas, although at much shorter time-scales and not necessarily reaching full equilibrium or homogeneity throughout the furnace volume. Conceptually, we see the ore as the protolith or parent material of the forming slag and metal. Slag formation is similar to the formation of magma when rock units are exposed to sufficient heat. As in magma development, the slag composition changes as a result of absorption and withdrawal of solid material while the process continues. In metal smelting, the ore charge melts almost completely as it travels down the furnace shaft towards the combustion zone in front of the tuyère, aided by the fluxing effect of the fuel ash and the absorption of varying amounts of ceramic material from the furnace (Rehren *et al.*, 2007 and references therein). Following the reaction in the lower parts of the furnace between the carbon monoxide generated by the incomplete combustion of the charcoal and the relevant metal oxides in the charge, a chemically well-defined metal phase forms and separates from the siliceous melt, thus changing the initial bulk composition of the charge to that of the residual melt phase, the slag. Thus, iron metal and several other elements which can be reduced to metal under the conditions prevailing in the furnace, such as copper, nickel, phosphorous or arsenic, are partly removed from the melt system. All other oxides, particularly silica, alumina, titania and the alkali and alkali earth oxides, summarised as non-reducible compounds (NRC), remain in the slag, together with a certain amount of iron oxide which is needed as a flux for the NRCs. The reconstruction of the smelting process is then based on the interpretation of chemical differences and similarities between the ore, slag, furnace wall material, fuel ash, as well as the metal produced. The more these various materials can be described chemically, the higher the potential to reconstruct details of the overall process.

3.2. Ore

The chemistry of the ore shows a significantly higher iron oxide content (72 to $\sim$80 wt%) as compared to the slag samples, whereas SiO_2 (*ca.* 14–18 wt%), Al_2O_3 (*ca.* 4–7wt%), and CaO (*ca.* 0.2 to $\sim$0.4 wt%) are much lower. In contrast, the content of P_2O_5 is relatively high (around 1 wt%). All the other elements except for TiO_2 (*ca.* 0.5 wt%) are present at rather low concentrations only, including MnO (below 0.1 wt%). Among the trace elements, Co (*ca.* 110–170 ppm), Zr (*ca.* 150 ppm), and Ba (*ca.* 100 ppm) stand out. Significantly, the copper content is negligible, at less than 50 ppm, ruling out the possibility that this ore could have been used to smelt copper; instead, it is an iron ore suitable for the traditional bloomery process.

Mineralogically, the ore is composed of angular quartz particles embedded in a matrix of haematite and goethite in repetitive layers. One sample (315a 1) shows a thin kaolinitic vein. Starting from this vein, haematite and goethite are forming spheroidal structures. This is a structure typical of concretions forming during iron enrichment by weathering. An iron crust of this type can form as part of a gossan (iron cap) or as lateritic weathering crust; differentiation between these two types is very difficult (Schwarz, 1992). As a general rule, an elevated base metal content, in the order of hundreds of ppm of copper, lead, zinc or nickel are indications for a gossan formed above a sulphidic ore deposit; in the ore samples analysed here, only 40–50 ppm copper, less than 100 ppm zinc and no lead were found by XRF analysis, so that a gossan formation seems unlikely. Laterites are defined by the ratio $SiO_2/(Al_2O_3+Fe_2O_3)$ (according to Schellmann, 1982). For formal laterite identification, it is necessary that this ratio is lower in the laterite than the ratio in the parental rock. In our case the parental rock was not available for analysis, but based on the appearance of the ore and the wider context, we assume that the best explanation

for the formation of the iron-rich crust represented by the ore samples in this region is lateritisation. A Mesozoic laterite horizon is known to occur in the surrounding area (Tadesse, 1997), and could be the source for the used ore.

3.3. Furnace slag

The main chemical components of the three analysed furnace slag samples are FeO (*ca.* 53–55 wt%), SiO_2 (*ca.* 33–35 wt%), and Al_2O_3 (*ca.* 6–7 wt%). The remaining elements are below 1 wt%, with the exception of CaO (*ca.* 2–2.5 wt%). The trace elements are ranging from 20 to 25 ppm (Zn) to >400 ppm (Zr). Significantly, the copper content reaches only 30–50 ppm, similar to that found in the ore samples and far too low to relate this material to copper smelting. The relative proportions of FeO, SiO_2, and Al_2O_3 are typical for fayalitic iron smelting slag (*e.g.*, Bachmann, 1982; Kronz, 1997; Miller & Killick, 2004).

The thin sections show fayalite (about 80–90 area %) as the main constituent in a glassy matrix. The olivine appears in two forms, as fine needles and as more developed crystals, with sizes ranging from 5 to 50–100 μm, indicative of variable cooling rates for the different parts of the samples (Donaldson, 1976). Such differences in grain size within and between samples reflect the non-equilibrium conditions which are characteristic for the crystallisation of archaeological slags. The second phase is dendritic to hypidiomorphic spinel, covering about 10 area % of the thin sections, in some cases forming accumulations or clusters. As shown by their Al-rich composition, they are a solid solution of hercynite and magnetite. Sample 302c shows a core of wüstite overgrown by a rim of spinel (Fig. 6a–d). The wüstite is marked by the high content in iron (Fig. 6a), surrounded first by a thin chromium-rich layer (Fig. 6b), followed by a thicker crust enriched in titanium, that is an iron-dominated spinel with a significant ulvitic component (Fig. 6c). The apparent Al-enrichment
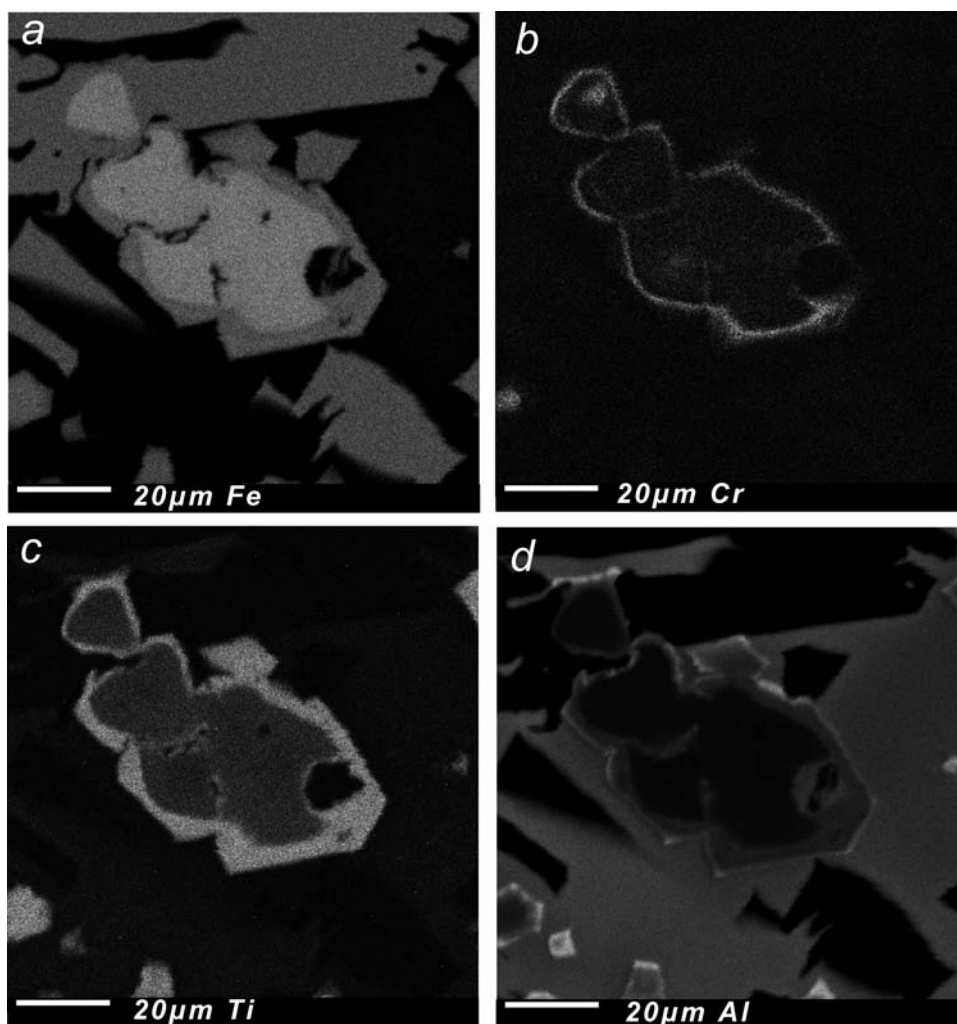
Fig. 6. X-ray maps for selected elements by EPMA, showing complex zoned iron oxide-rich particles in a matrix of fayalite and glass; sample 302c. (a) The core of the particle consists of wüstite (light grey, indicating highest Fe concentration), surrounded by a less iron-rich material (medium grey). The medium grey crystals above, left of, and below the central grain are fayalite. (b) A very thin layer rich in chromium starts the spinel formation. (c) The bulk of the spinel is rich in titanium. (d) Aluminium is more enriched in the surrounding glass (medium grey) than in the spinel phase (dark grey), and virtually absent from the wüstite and fayalite (both black).

at the very end of the crystallisation is remarkable, indicating that for much of the formation period the uptake of aluminium into the spinel was limited at a level below the available aluminium in the surrounding melt (Fig. 6d), while titanium strongly partitions into the spinel phase. This is underlined by the higher aluminium level visible in the glass phase (light grey in Fig. 6d) as compared to the aluminium level in the spinel (darker grey), and the strong enrichment of titanium (light grey in Fig. 6c) in the spinel only. This is in good agreement with the miscibility gap in the system hercynite-ulvöspinel (Muan *et al.*, 1972; Knecht *et al.*, 1979). The concentration of chromium in the first phase of spinel formation (Fig. 6b) is also consistent with its known geological behaviour, resulting in strong partitioning of this element in the early forming spinels as seen for instance in the formation of chromite deposits during the early crystallisation of basic magmas. Table 2 gives EPMA data for cores and rims of zoned spinels from samples 314a and 316, showing in general increased TiO_2 and lower Al_2O_3 contents in rims compared to cores, although for Al_2O_3 also the opposite can be found (*e.g.*, 314a-4 and 316-2).

In different furnace slag samples, small clusters of rounded iron oxide were found, identified by their shape, optical properties and composition as wüstite (Fig. 7). In addition, a small particle of metallic iron, partly transformed to iron hydroxide, was found in sample 302c (Fig. 8).

After the crystallisation of fayalite, wüstite and spinel, the remaining melt consolidates as glass, filling in the interstitial spaces (Fig. 7). This melt represents the lowest liquidus composition of the system and is enriched in those compounds that are not or only partly compatible with the crystallising phases, such as K_2O, Al_2O_3, P_2O_5, SiO_2, and CaO. The glass matrix shows a two- to four-fold increase in the concentration of these oxides as compared to the bulk composition (Al_2O_3 increases from *ca.* 7 wt% in the bulk composition to *ca.* 14 wt% in the glass, P_2O_5 from *ca.* 0.2 to *ca.* 0.8 wt%, K_2O from *ca.* 0.3–0.9 wt%,

and CaO from *ca.* 2.5–8 wt%). At the same time, the FeO concentration is much lower in the glass phase as compared to the bulk composition, down from *ca.* 54 wt% to only 23 wt% (Table 3).

3.4. Tap slag

The tap slag is chemically very similar to the furnace slag across all major and minor oxides and trace elements, but with a slight tendency towards higher and more varied FeO contents. In the ternary phase diagram, both slag types plot along the eutectic trough in the fayalite field, indicating a furnace temperature of approximately 1150 °C (Fig. 9). The content of copper varies between 25 and 50 ppm, consistent with the furnace slag and by far insufficient to allow linking this slag to copper metallurgy.

The main mineral phase in the tapped slag is fayalite, but in the form of smaller and much more elongated crystals compared to those seen in the furnace slag, suggesting a more rapid cooling (Donaldson, 1976). The crystal needles near the surface are orientated perpendicular to the surface, forming a spinifex texture typical of tap slag (*e.g.*, Müller *et al.*, 1988). Spinel is the second most common phase, with most of the crystals showing zoning from an aluminium-richer core to a rim of titanium-rich spinel with only limited aluminium uptake at the end, resulting in enrichment of aluminium in the surrounding melt (see also Knecht *et al.*, 1979).

No wüstite was found in any of the studied samples of tap slag, in contrast to the furnace slag. However, the flow surface of the tap slag is marked by a dense skin of minute magnetite crystals. These form due to the oxidation of Fe^{2+} at the contact area between the hot melt surface and ambient air when the slag is tapped from the furnace. This leads to an assimilation of oxygen into the melt and an increased Fe^{3+} supply, resulting in the formation of magnetite at the expense of hercynite. The band of magnetite and the

Table 2. EPMA analyses of zoned spinel crystals in slag samples from Aksum, Ethiopia, reported in wt%. Spot analyses of arbitrarily selected zoned grains, measured at 15 kV and 20 nA. Note that these analyses do not relate to the complex grain shown in Fig. 6.

|	MgO	Al_2O_3	SiO_2	TiO_2	Cr_2O_3	FeO	Total
314a-1-core	0.05	21.4	0.57	7.0	0.44	66.4	95.9
314a-1-rim	0.06	11.9	0.78	7.3	0.73	73.8	94.9
314a-4-core	0.11	6.4	0.38	2.0	0.09	86.3	95.5
314a-4-rim	0.08	12.6	0.46	8.7	0.58	72.1	94.7
314a-5-1-core	0.35	30.7	0.47	4.2	2.42	59.0	97.3
314a-5-1-rim	0.12	11.5	0.83	6.2	1.13	75.8	95.6
314a-5-2-core	0.33	44.4	0.34	1.8	2.67	49.2	98.7
314a-5-2-rim	0.10	13.1	0.51	6.3	0.64	75.2	96.1
316-2-core	0.09	6.4	0.43	2.5	0.13	85.1	94.8
316-2-rim	0.12	13.7	0.58	7.4	0.98	71.5	94.4
316-3-1-core	0.17	34.8	0.45	3.4	0.27	59.5	98.8
316-3-1-rim	0.09	11.8	0.72	7.8	0.34	73.9	94.7
316-3-2-core	0.20	41.0	0.46	3.1	0.32	53.9	99.2
316-3-2-rim	0.06	23.3	1.74	6.2	0.01	66.3	97.9
316-3-2-rim	0.09	13.3	0.79	7.1	0.60	73.3	95.4
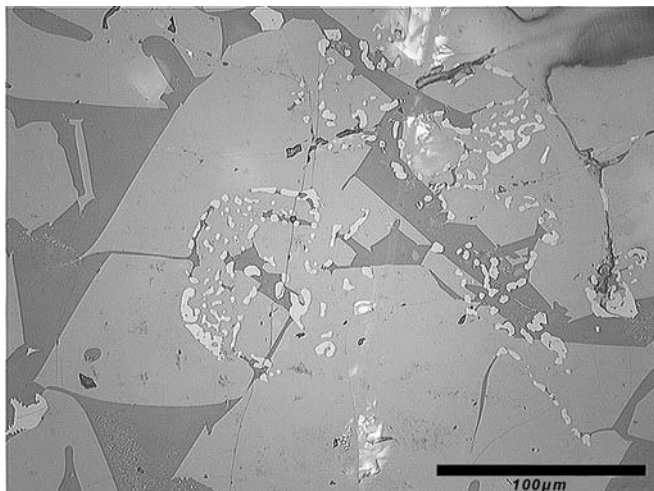
Fig. 7. Photomicrograph taken in reflected polarised light illustrating a cluster of wüstite particles (light grey) in fayalite (angular) and in the glassy matrix (dark grey). Furnace slag, sample 302c.
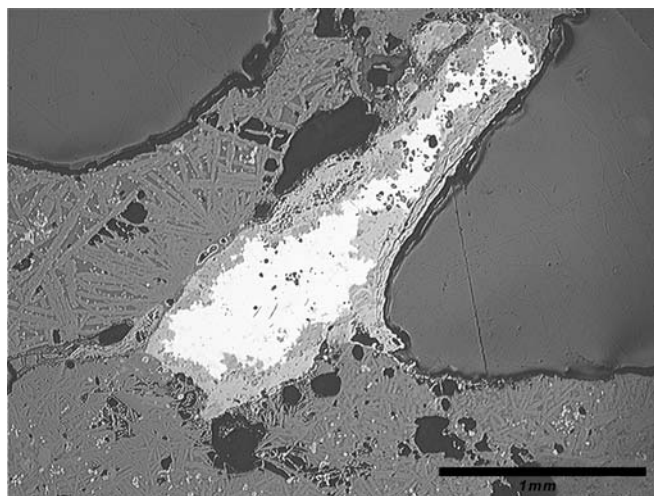
Table 3. EPMA analyses of the interstitial glass, sample 302c, reported in wt%. Spot analyses, measured at 15 kV and 20 nA.

	Na_2O	Al_2O_3	SiO_2	P_2O_5	K_2O	CaO	FeO	Total
#1	0.52	14.2	50.7	0.82	0.92	8.06	23.1	98.4
#2	0.59	14.8	48.8	0.77	0.74	8.64	24.6	98.8
#3	0.36	13.8	45.5	0.73	0.78	8.12	27.8	97.1
#4	0.44	13.7	51.8	0.86	0.85	8.06	22.0	97.7
#5	0.36	13.4	43.5	0.69	1.17	5.91	30.4	95.4
#6	0.71	18.3	51.0	0.88	0.79	9.83	12.5	94.1
#7	0.60	14.8	45.7	0.78	0.63	7.65	26.5	96.7

Fig. 8. Metallic iron (bright white) surrounded by corrosion products (light grey) and very fine-grained needle-like fayalite crystals. The black irregular parts represent porosity. Furnace slag, sample 302c.
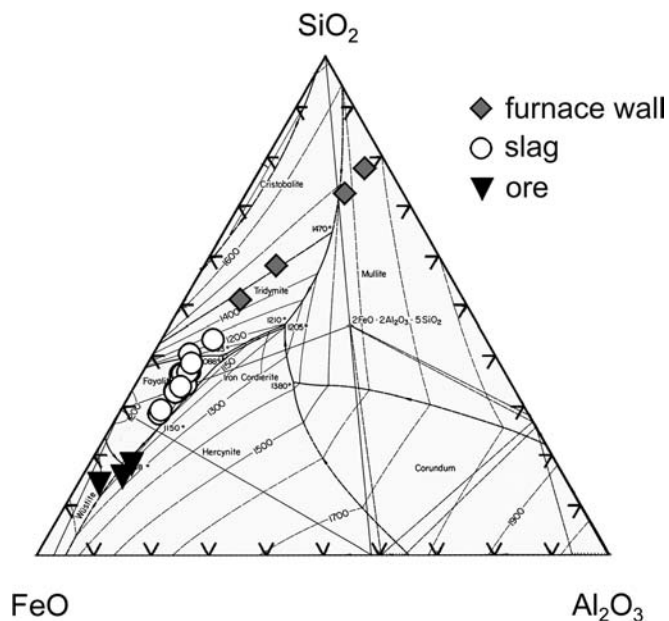
Fig. 9. Projection of the analysed samples into the ternary liquidus phase diagram $FeO – Al_2O_3 – SiO_2$. Two of the samples (313g.1 and 313g.2) labelled ''furnace wall'' are mixtures of slag and furnace wall material, and therefore fall into relatively high-silica regions atypical for bloomery slag.

overall shape of the samples are further evidence for a slag tapping out of the furnace in liquid form. This is also consistent with the observed characteristics in grain size, habit, and texture, which all strongly indicate a much more rapid cooling of the slag (Müller *et al.*, 1988), and in contact with ambient air, as compared to the furnace slag which cooled more slowly within the furnace and its more reducing atmosphere.

In some cases the fayalite shows a conversion into an opaque phase, which is attributed to an oxidation process. This can be a result of the latest stage of solidification at increased oxygen supply, when the non-compatible Fe^{3+} ions in the melt are sufficiently enriched to trigger the formation of ferri-fayalite or laihunite, or due to weathering of the slag over long periods of time (*e.g.*, Moesta & Schlick, 1989; Moesta *et al.*, 1989; Metten, 2003).

3.5. Furnace wall material

Some samples of slag show the effect of incorporated furnace wall material (see Fig. 5). These samples show a chemical composition with a clear mixing line extending from the fayalitic furnace slag towards higher SiO_2 and Al_2O_3 values (Fig. 9). In the extreme cases, the samples reach in part values of more than 70 wt% for SiO_2 and 16 wt% for Al_2O_3; these are pure furnace wall material. At the same time, the content of iron oxide is as low as 3–4 wt%. The values of CaO (up to 4 wt%), K_2O (around 3 wt%), and Na_2O (*ca.* 2 wt%), as well as barium (about 1000 ppm) are all higher than the pure slag samples. Sample 313f, which shows already macroscopically the largest amount of furnace wall material, presents the highest contents of SiO_2, Al_2O_3, Ka_2O, Na_2O, and Ba in the bulk analysis.

4. Discussion

4.1. Copper or iron smelting?

Both iron and copper smelting were well developed in many parts of Africa since at least the late first millennium B.C., as indicated by the regular occurrence of production remains as well as copper and iron objects in the archaeological record (Tylecote, 1982; Childs & Killick, 1993; Miller *et al*., 2001; Miller, 2002; Miller & Killick, 2004). For Aksum, well connected in the 4th century A.D. with major foreign powers such as India and the Byzantine Empire, both metals would have been additionally available via trade routes. Thus, the existence of copper or bronze artefacts in Aksum does not in itself provide evidence for local copper smelting; however, nor can such a metallurgy be ruled out *a priori*.

The differentiation of archaeological remains resulting from pre-industrial iron and copper smelting is not necessarily straightforward. Both regularly produce a very iron-rich fayalitic slag, with typically 60–70 wt% FeO and around 20–30 wt% SiO_2; the balance to 100 wt% being minor oxides such as Al_2O_3, CaO, and TiO_2 as well as various trace elements (Bachmann, 1982; Craddock, 1995). These slags are well known from numerous archaeometallurgical studies (for iron see Rehren *et al*., 2007 and references therein, for copper see Hauptmann, 2009 and references therein), corroborating the fundamental compositional similarity of copper and iron smelting slag across many societies. However, some mineralogical and chemical indicators allow distinguishing them. Miller & Killick (2004, p. 34) state that in ''copper smelting slag free iron oxide is present as magnetite, not wüstite, in most cases''. This difference reflects the different redox conditions required for smelting copper and iron; the reduction of copper oxide to copper metal takes place under conditions where magnetite is stable, while the reduction of iron oxide to iron metal requires much more reducing conditions, where wüstite is the stable free iron oxide. A recent study by Muralha *et al*. (2011) showed how predominant wüstite can coexist with hercynitic spinel and residual magnetite from the ore in the same piece of iron slag, reflecting redox gradients and non-equilibrium conditions often found in ancient metallurgy. Furthermore, Miller & Killick (2004) report examples of pre-industrial copper smelting slags from southern Africa with typical concentrations of 0.5–1 wt% Cu_2O, which is consistent with archaeological copper smelting slags from much of Europe and the Middle East (Bachmann, 1982; Craddock, 1995).

Both the ore samples and the slag from Aksum have copper contents of less than *ca.* 50 ppm. Free iron oxide is relatively rare in the slag samples; where present, it is predominantly wüstite as in the furnace slag, or magnetite which formed only during the tapping of the slag as a thin skin on the oxidised surface. The primary spinels found in the slag are predominantly hercynite and ulvöspinel, and have only little Fe^{3+} component. Therefore, we argue that all samples analysed here are consistent with iron smelting using the bloomery process (Craddock, 1995), but not the copper smelting initially suggested by the excavator of these samples.

4.2. Ore to slag relationship

The occurrence of iron ore fragments among the archaeological finds enabled us to compare their composition to the slag (Table 1), in order to test whether this ore could have provided the charge for the furnaces from which the slag found here originated. For this, we compared the minor oxides and trace element concentrations of the two materials, assuming that during smelting the furnace charge is depleted in iron, while all other non-reducible compounds increase proportionally in the remaining slag melt. Of course, even a perfect match would not be proof that *this* ore was indeed used to produce *this* slag; however, major discrepancies would more or less rule out such a possible link. For this exercise, we selected the most iron-rich ore sample 315a-1, assuming that the pieces found among the waste material were deliberately discarded by the head smelter, and that the average ore used is more akin to the best rather than to the average of the waste. The other two ore samples were also considered, but only qualitatively.

Inspection of the data in Table 1 shows that for many NRCs the concentrations in the slag are consistently about twice those in the ore (SiO_2, Al_2O_3, TiO_2, Zr, Ba), while the iron content is much lower in the slag, as expected. Some discrepancies from this pattern, however, are also apparent. MgO, K_2O, CaO and Sr are significantly enriched, by up to a factor of nearly ten, while manganese, cobalt, copper, zinc and phosphorous are present at roughly the same or even lower concentrations in the slag as in the ore respectively. These differences, however, are fully consistent with the assumed bloomery smelting process. The first group of elements is characteristic of fuel ash from wood (Wedepohl, 1998) and the charcoal made from such wood, and its increased presence in the slag is most likely due to the fuel ash being absorbed by the slag during smelting (Crew, 2000). In contrast, the elements not enriched or even depleted are all known to partition into the metallic iron during bloomery smelting, and are thus removed from the system together with the bloom. Thus, we may conclude that the analysed ore pieces are most likely similar to the ore that was smelted here.

In many societies, iron smelting furnaces are designed in such a way that the ceramic material from furnace walls or tuyère provides a contribution to the slag-forming process, effectively acting as a flux (Veldhuijzen & Rehren, 2007 and references therein). Assessment of the data in Table 1 suggests that this has not been the case in 3rd to 4th century A.D. Aksum. The analyses of the technical ceramic fragments (Table 1, samples 313f and 314) and of slag mechanically mixed with ceramic (samples 313g.1 and 313g.2) are all characterised by relatively high concentrations of barium, reaching 1000 ppm in the pure ceramic. In

contrast, the slag has only around 150–200 ppm barium, about twice as much as the ore (see Table 1) and in line with the generally observed enrichment factor for non-reducible components from the ore. Any significant addition of ceramic material to the slag would have resulted in an increased barium concentration in the slag, as shown in the two samples 313g.1 and 313g.2 of mechanically mixed slag and furnace wall material. The absence of such a barium increase in the furnace and tap slag over and above the enrichment due to the removal of substantial quantities of iron oxide from the system indicates that the ceramic material of the furnace contributed little if any material to the slag. This shows that the ore used was self-fluxing and that absorption of furnace wall material into slag was restricted to the immediate contact zone between the two.

4.3. Proficiency and productivity

So far, this paper has focussed on the chemical and mineralogical reconstruction of the metal smelting process, but has provided little information of direct archaeological relevance beyond the identification of iron smelting as the source for this slag. For a better understanding of the role which this process may have played within the site from where the material was recovered, it is important to gain an understanding of the proficiency with which it was conducted, and at which scale – was it an *ad hoc* small-scale process to serve local needs, or a more regular production, possibly serving a larger area? This would have implications for the understanding of whether the smelting was done by part- or full-time specialists, or by less proficient farmers or hunters. To reach this level of archaeometric interpretation it would be necessary to have a more complete picture of the situation on site, including an estimate of the amount of slag produced and the length of time over which it accumulated. In the absence of such data we present here just some sample estimates to demonstrate the potential utility of such analyses for a wider archaeological interpretation. This assessment, of course, is only tentative, since we have no way to determine how representative the few analysed samples are for all the material processed at the site.

It is notable that the examined furnace and tap slag samples are consistently very poor in wüstite, which means they are very lean slag as compared to many broadly contemporary European slags which often have substantial amounts of wüstite (Oelsen & Schürmann, 1954; Schürmann, 1958; Pleiner, 1980, 2000; Kronz, 1997). The formation of such a lean slag can be due to two reasons, either strongly reducing conditions in the furnace, or a dilution of the ore through absorption of furnace wall material (Rehren *et al.*, 2007). We have shown above that there was only very little if any contribution from the furnace wall ceramic to the slag formation, indicating that the smelting conditions here were very strongly reducing and the process designed to maximise metal extraction. That would imply a high fuel to ore ratio, that is a

relatively high consumption of charcoal during smelting, resulting in a very high ratio of carbon monoxide to carbon dioxide within the furnace atmosphere (Craddock, 1995). Such conditions not only increased metal yield, but also resulted often in the absorption of carbon in the metal, that is the formation of steel instead of soft iron. The possible reduction of manganese and phosphorous as a metallic phase into the metal, deduced from their lack of enrichment in the slag compared to the ore, is consistent with such a scenario, and would constitute further evidence for the theory arguing that in Africa steel was commonly obtained by the direct process (van der Merwe & Avery, 1982; Hahn, 1993). Overall, we interpret these observations as indicating that at Aksum, the bloomery process was conducted very proficiently, and therefore probably by specialised smelters. But what about the scale of production?

The analytical data enable a rough mass balance estimation even though no absolute values for the amount of slag present at the furnace site are known. We have shown above that the slag formed from the accumulation of NRCs with some added fuel ash, but no further ceramic contribution. We also have indications about the contents of iron oxide in the ore (*ca.* 80 wt% FeO) and the slag (*ca.* 55–60 wt% FeO). For the sake of argument we set the ore concentration at 80 wt% iron oxide, with the remaining 20 wt% being made up predominantly of NRCs. For the slag, we assume 40 wt% NRCs from the ore, plus a few additional percent of fuel ash, leaving between 55 and 60 wt% iron oxide. Thus, 100 kg of this slag contains 40 kg of NRCs from the ore. To obtain that much NRC material, one needs 200 kg of ore of the defined quality. These 200 kg of ore contain also 160 kg of iron oxide, of which (calculating generously) 60 kg remain in the slag. Thus, 100 kg of iron oxide has been extracted from the ore in the form of iron metal; using the conversion factor of 0.77 from FeO to Fe shows that about 77 kg of iron metal were extracted as bloom iron. The bloom needs further processing into bar or billet form before it can be shaped into artefacts. The smithing results in a considerable but highly variable loss of metal (Crew, 1991). Consequently, the smelter may have obtained around 50 kg of useful iron metal for each 100 kg of slag they produced. Alternatively, one could argue that the ore analysed here was of mediocre quality, and that 90 wt% iron oxide is a more realistic approximation for the quality of the smelted ore. The same estimation would then indicate that in order to accumulate 40 kg of NRCs that are present in each 100 kg of slag, 400 kg of ore would be needed. In this scenario, 360 kg of iron oxide would be added to the furnace charge, and still only 60 kg retained as slag. Thus, 300 kg of iron oxide were available to be reduced to metal, equivalent to about 230 kg of bloomery iron. Allowing for the inevitable smithing loss, this would probably be something like 150 kg of useful metal. In summary, we argue that it is reasonable to assume that the amount of useful metal that was produced in this process was similar to the amount of slag left behind, with a potential error of ± 50 %. Unfortunately, in the case presented here the quantity of slag preserved at

the site is not known. However, it is hoped that the discussion above demonstrates that it is worthwhile to document the quantity of slag present in archaeological sites, and to conduct comprehensive analyses of all relevant materials.

5. Conclusion

The analysis of 19 slag, ore and furnace wall samples dated to the late 3rd and early 4th century A.D. and originating from an archaeological excavation in Aksum, Ethiopia, has failed to confirm the suspected copper smelting. The concentration of copper, determined by XRF analysis, is less than 50 ppm in all ore and slag samples, while typical prehistoric copper slags have at least around 2000 to normally more than 5000 ppm Cu. In addition, the mineralogical investigation confirmed the presence of metallic iron in some of the slag, but failed to identify either metallic copper or copper sulphide, phases which are inevitably present in ancient copper slag. Also, the redox conditions as deduced from the presence of various free iron oxides point to strongly reducing conditions in line with bloomery iron smelting, but exceeding by far those necessary and common for copper smelting. Thus, it is beyond reasonable doubt that these samples originated from iron smelting using the bloomery process. The very low level of free iron oxide in all slag samples and the concentration pattern for certain trace elements indicate that the produced metal was more likely steel than soft iron, in keeping with other observations relating to African iron production elsewhere.

There is very little need to assume a substantial contribution from the furnace wall to the slag formation, suggesting that the visually observed mixing of vitrified furnace wall material and smelting slag is restricted to the immediate contact zone between slag melt and furnace wall.

Several oxides such as CaO, MgO and K_2O show a much higher enrichment factor in the slag compared to the ore. This can be explained by the fact that these oxides are highly enriched in wood ash, and therefore most likely originate from the charcoal. Overall, the chemical relationship between ore, slag and fuel ash suggests that the slag could well have formed from the smelting of a self-fluxing lateritic ore very similar to that found on site.

The lack of any data on the amount of slag present at Aksum makes it difficult to discuss the scale of production. However, a comparison of the composition of the ore, slag and furnace wall material allows us to comment on the relative efficiency of the process in relation to iron extraction, and to postulate a factor of 1 ± 0.5 that can be applied to the amount of slag present, to estimate the amount of iron metal produced per unit of slag. It is hoped that future work at this important archaeological site will be able to quantify the amount of slag present. This can then be used in combination with further dating evidence to estimate the annual iron output, providing information whether the smelting activity served only the immediate needs of the inhabitants of the settlement, or supplied iron for a larger community.

References

Bachmann, H.-G. (1982): The identification of slags from archaeological sites, Institute of Archaeology Occasional Paper 6. Institute of Archaeology, London, 37 p.

Childs, T. & Killick, D. (1993): Indigenous African metallurgy: nature and culture. *Rev. Anthropol.*, **22**, 317–337.

Craddock, P. (1995): Early metal mining and production. Edinburgh University Press, Edinburgh, 363 p.

Crew, P. (1991): The experimental production of prehistoric bar iron. *Hist. Metall.*, **25**, 21–36.

Crew, P. (2000): The influence of clay and charcoal ash on bloomery slags – A contribution to the quest of the Holy Grail. *in* ''Iron in the Alps: deposits, mines and metallurgy from antiquity to the XVI century'', C. Cucini Tizzoni & M. Tizzoni, eds., Breno, Commune di Bienno, 38–48.

Donaldson, C.H. (1976): An experimental investigation of olivine morphology. *Contrib. Mineral. Petrol.*, **57**, 187–213.

Hahn, H.P. (1993): Eisentechniken in Nord-Togo, Kulturanthropologische Studien 21. LIT Verlag, Hamburg, 170 p.

Hauptmann, A. (2009): The Archaeometallurgy of Copper: Evidence from Faynan, Jordan. Springer, Berlin, Heidelberg, New York, 388 p.

Knecht, B., Woermann, E., El Goresy, A. (1979): Element distributions among spinel and ilmenite phases in the systems FeO-Cr_2O_3-TiO_2, FeO-Al_2O_3-TiO_2 and FeO-MgO-TiO_2. *Lunar Planet. Sci. Lett.*, **10**, 670–672.

Kronz, A. (1997): Phasenbeziehungen und Kristallisationsmechanismen in fayalitischen Schmelzsystemen – Untersuchungen an Eisen- und Bundmetallschlacken. Klaus Bielefeld Verlag, Friedland, 275 p.

Metten, B. (2003): Beitrag zur spätbronzezeitlichen Kupfermetallurgie im Trentino (Südalpen) im Vergleich mit anderen prähistorischen Kupferschlacken aus dem Alpenraum. *Metalla*, **10**, 1–122.

Miller, D. (2002): Smelter and smith: iron Age metal fabrication technology in southern Africa. *J. Archaeol. Sci.*, **29**, 1083–1131.

Miller, D. & Killick, D. (2004): Slag identification at southern African archaeological sites. *J. Afr. Archaeol.*, **2**, 23–47.

Miller, D., Killick, D., van der Merwe, N.J. (2001): Metal working in the northern Lowveld, South Africa, A.D. 1000–1890. *J. Field Archaeol.*, **28**, 401–417.

Moesta, H., Rüffler, R., Schnau-Roth, G. (1989): Zur Verfahrenstechnik der bronzezeitlichen Kupferhütten am Mitterberg, Mößbauer und mikroskopische Studien. *in* ''Archäometallurgie der alten Welt/ Old World archaeometallurgy'', A. Hauptmann, E. Pernicka., G. Wagner, eds., Der Anschnitt Beiheft **7**, Deutsches Bergbau-Museum, Bochum, 141–153.

Moesta, H. & Schlick, G. (1989): The furnace of Mitterberg – an oxidizing Bronze Age copper process. *Bull. Metal. Mus.*, **14**, 5–16.

Muan, A., Hauck, J., Löfall, T. (1972): Equilibrium studies with a bearing on lunar rocks. i Proceedings of the third lunar science conference, Supplement 3, *Geochim. Cosmochim. Acta*, **1**, 185–196.

Munroe-Hay, S.C.H. (1991): Aksum: an African civilisation of late antiquity. Edinburgh University Press, Edinburgh, 294 p.

Muralha, V.S.F., Rehren, Th., Clark, R.J.H. (2011): Characterization of an iron smelting slag from Zimbabwe by Raman microscopy and electron beam analysis. *J. Raman Spectr.*, doi: 10.1002/jrs.2961.

Müller, G., Schuster, A.K., Zippert, Y. (1988): Spinifex textures and texture zoning in fayalite-rich slags of medieval iron-works near Schieder Village, NW-Gemany. *N. Jb. Miner. Mh.*, **1988**, 111–120.

Oelsen, W. & Schürmann, E. (1954): Untersuchungsergebnisse alter Rennfeuerschlacken. *Arch. Eisenhüttenw.*, **25**, 507–514.

Pleiner, R. (1980): Early iron metallurgy in Europe. *in* ''The Coming of the Age of Iron'', T.A. Wertime & J.D. Muhly, eds., Yale University Press, New Haven, CT, 375–415.

Pleiner, R. (2000): Iron in archaeology: the European bloomery smelters. Archeologický Ústav AVČR, Prague, 400 p.

Rehren, Th. (2001): Meroe, iron. *MittSAG*, **12**, 102–109.

Rehren, Th., Charlton, M., Chirikure, Sh., Humphris, J., Ige, A., Veldhuijzen, A.H. (2007): Decisions set in slag – the human factor in African iron smelting. *in* ''Metals and Mines – Studies in Archaeometallurgy'', S. La Niece, D. Hook, P. Craddock, eds., Archetype, London, 211–218.

Schellmann, W. (1982): Eine neue Laterit definition. *Geol. Jahrb.*, **58**, 31–47.

Schwarz, T. (1992): Produkte und Prozesse exogener Fe-Akkumulationen: Eisenoolithe und lateritische Eisenkrusten im Sudan. PhD dissertation, TU Berlin, 186 p.

Schürmann, E. (1958): Die Reduktion des Eisens im Rennfeuer. *Stahl und Eisen*, **19**, 1297– 1308.

Sperl, G. (1980): Über die Typologie urzeitlicher, frühgeschichtlicher und mittelalterlicher Eisenhüttenschlacken. Studien zur Industrie-Archäologie 7. Österreichische Akademie der Wissenschaften, Wien, 68 p.

Tadesse, T. (1997): The geology of Axum area. Memoir No. 9, Ethiopian Institute of Geological Survey, Addis Ababa, 184 p.

Tylecote, R. (1982): Early copper slags and copper-base metal from the Agadez Region of Niger. *Hist. Metall.*, **16**, 58–64.

van der Merve, N.J. & Avery, D.H. (1982): Pathway to steel. *Am. Sci.*, **70**, 146–155.

Veldhuijzen, H.A. (2003): 'Slag_Fun' – a new tool for archaeometallurgy: development of an analytical (P)ED -XRF method for iron rich materials. *Papers From Inst. Archaeol.*, **14**, 102–118.

Veldhuijzen, H.A. (2005): Early iron production in the Levant. PhD dissertation, University of London, 327 p.

Veldhuijzen, H.A. & Rehren, Th. (2007): Slags and the city: early iron production at Tell Hammeh, Jordan, and Tel Beth-Shemesh, Israel. *in* ''Metals and Mines – Studies in Archaeometallurgy'', S. La Niece, D. Hook, P. Craddock, eds., Archetype, London, 189–201.

Wedepohl, K.H. (1998): Mittelalterliches Glas in Mitteleuropa: Zusammensetzung, Herstellung, Rohstoffe. *Nachrichten Der Akademie Der Wissenschaften in Göttingen, II Mathematisch-Physikalische Klasse*, **1**, 5–56.

Ziegert, H. (2001): Preliminary report on the Hamburg archaeological mission to Axum 2000. *Annales d'Ethiopie*, **17**, 135–146.

Ziegert, H. (2006): Aksum – Quarries and copper processing. *in* ''Proceedings of the XVth International Conference of Ethiopian Studies, Hamburg July 20–25, 2003'', S. Uhlig, ed., *Aethiopische Forschungen,* 65, Harrassowitz Verlag, Wiesbaden, 396–400.

Ziegert, H. (2009): *[14]C-Dating and volcanism.* Available at: http://www1.uni-hamburg.de/helmut-ziegert/pdf/publications/HZiegert-14CandVolcanism(2009).pdf.